

Estimation of the Optical Constants and the Thickness of Thin Films Using Unconstrained Optimization

Ernesto G. Birgin,* Ivan Chambouleyron,† and José Mario Martínez*

*Department of Applied Mathematics, IMECC-UNICAMP, CP 6065, CEP 13081-970, Campinas, SP, Brazil;

†Department of Applied Physics, IPGW-UNICAMP, CP 6065, CEP 13083-970, Campinas, SP, Brazil

E-mail: ernesto@ime.unicamp.br, ivanch@ifi.unicamp.br, martinez@ime.unicamp.br

Received May 5, 1998; revised November 23, 1998

The problem of estimating the thickness and the optical constants of thin films using transmission data only is very challenging from the mathematical point of view and has a technological and an economic importance. In many cases it represents a very ill-conditioned inverse problem with many local-nonglobal solutions. In a recent publication we proposed nonlinear programming models for solving this problem. Well-known software for linearly constrained optimization was used with success for this purpose. In this paper we introduce an unconstrained formulation of the nonlinear programming model and we solve the estimation problem using a method based on repeated calls to a recently introduced unconstrained minimization algorithm. Numerical experiments on computer-generated films show that the new procedure is reliable. © 1999 Academic Press

Key Words: unconstrained minimization; spectral gradient method; optical constants; thin films.

1. INTRODUCTION

For most modern applications of thin dielectric or semiconductor films, the optical properties of interest cover a photon energy range around the fundamental absorption edge of the material. Moreover, as the applications make use of multiple coherent reflections at the interfaces, the thickness of the films is an important design and characterization parameter. Optical transmittance provides accurate and rapid information on the spectral range where the material goes from complete opacity to some degree of transparency [1, 2]. As a consequence, the problem of retrieving the optical constants ($\tilde{n}(\lambda) = n(\lambda) + ik(\lambda)$) and the thickness (d) of thin films, from transmission data only, is of particular importance. Some useful approximate solutions have been found in cases where the transmittance displays an

interference pattern in a highly transparent spectral region [3–5]. Up to now, however, the general solution of the problem has been elusive, because the system of equations is highly undetermined. Recently, we reported a new method, based on a pointwise constrained optimization approach, which allows us to solve the general case [6, 7]. The method defines a nonlinear programming problem, the unknowns of which are the coefficients to be estimated, with linear constraints that represent prior knowledge about the physical solution. The retrieval of the correct thickness and optical constants of the films does not rely on the existence of interference fringes. The new method was successful in retrieving d and $\tilde{n}(\lambda)$ from very different transmission spectra of computer made and real world films [6, 7]. The main inconvenience of the pointwise constrained optimization approach [6, 7] is that it is a rather complex large-scale linearly constrained nonlinear programming problem whose solution can be obtained only by means of sophisticated and not always available computer codes that can deal effectively with the sparsity of the matrix of constraints [8, 9].

We consider then the problem of estimating the absorption coefficient, the refractive index and the thickness of thin films, using transmission data only. Given the wavelength λ , the refractive index of the substrate s , and the unknowns d (thickness), $n(\lambda)$ (refractive index), and $\kappa(\lambda)$ (attenuation coefficient), the theoretical transmission is given by a well-known formula [2, 4, 5]. Having measurements of the transmission at (many) different wavelengths we want to estimate the above mentioned unknowns. At a first glance, this problem is highly undetermined since, for each wavelength, the single equation

$$\text{theoretical transmission} = \text{measured transmission} \quad (1)$$

has three unknowns d , $n(\lambda)$, $\kappa(\lambda)$ and only d is repeated for all values of λ . The driving idea in [6, 7] was to incorporate prior knowledge on the functions $n(\lambda)$ and $\kappa(\lambda)$ in order to decrease the degrees of freedom of (1) up to a point that only physically meaningful estimated parameters are admitted.

The idea of assuming a closed formula for n and κ depending on few coefficients has already been reported [3–5]. The methods originated from this idea are efficient when the transmission curve exhibits a fringe pattern representing rather large spectral zones where $\kappa(\lambda)$ is almost null. In other cases, the satisfaction of (1) is very rough or the curves $n(\lambda)$ and $\kappa(\lambda)$ are physically unacceptable.

In [6, 7], instead of imposing a functional form to $n(\lambda)$ and $\kappa(\lambda)$, the phenomenological constraints that restrict the variability of these functions were stated explicitly so that the estimation problem took the form:

$$\begin{aligned} \text{minimize } & \sum_{\lambda} [\text{theoretical transmission}(\lambda) - \text{measured transmission}(\lambda)]^2 \quad (2) \\ & \text{subject to } \textit{Physical Constraints}. \end{aligned}$$

In this way, well behaved functions $n(\lambda)$ and $\kappa(\lambda)$ can be obtained without severe restrictions that may damage the quality of the fitting (1).

The main contribution of the present paper is to establish a method for solving the estimation problem where (2) is replaced by an unconstrained optimization problem. We solved this problem using a very simple algorithm introduced recently by Raydan [10]. This method realizes a very effective idea for potentially large-scale unconstrained minimization. It consists of using only gradient directions with steplengths that ensure rapid convergence. The reduction of (2) to an unconstrained minimization problem needed the calculation

of very complicated derivatives of functions, which could not be possible without the use of automatic differentiation techniques. Here we used the procedures for automatic differentiation described in [11].

2. UNCONSTRAINED FORMULATION OF THE ESTIMATION PROBLEM

The transmission T of a thin absorbing film deposited on a thick transparent substrate (see [4, 5]) is given by

$$T = \frac{A\mathbf{x}}{B - C\mathbf{x} + D\mathbf{x}^2}, \quad (3)$$

where

$$A = 16s(n^2 + \kappa^2), \quad (4)$$

$$B = [(n + 1)^2 + \kappa^2][(n + 1)(n + s^2) + \kappa^2], \quad (5)$$

$$C = [(n^2 - 1 + \kappa^2)(n^2 - s^2 + \kappa^2) - 2\kappa^2(s^2 + 1)]2 \cos \varphi - \kappa[2(n^2 - s^2 + \kappa^2) + (s^2 + 1)(n^2 - 1 + \kappa^2)]2 \sin \varphi, \quad (6)$$

$$D = [(n - 1)^2 + \kappa^2][(n - 1)(n - s^2) + \kappa^2], \quad (7)$$

$$\varphi = 4\pi nd/\lambda, \quad \mathbf{x} = \exp(-\alpha d), \quad \alpha = 4\pi\kappa/\lambda. \quad (8)$$

In formulae (4)–(8) the following notation is used:

- (a) λ is the wavelength;
- (b) $s = s(\lambda)$ is the refractive index of the transparent substrate (assumed to be known);
- (c) $n = n(\lambda)$ is the refractive index of the film;
- (d) $\kappa = \kappa(\lambda)$ is the attenuation coefficient of the film (α is the absorption coefficient);
- (e) d is the thickness of the film.

A set of experimental data $(\lambda_i, T^{meas}(\lambda_i))$, $\lambda_{\min} \leq \lambda_i < \lambda_{i+1} \leq \lambda_{\max}$, for $i = 1, \dots, N$, is given, and we want to estimate d , $n(\lambda)$, and $\kappa(\lambda)$. This problem seems highly underdetermined. In fact, for known d and given λ , the following equation must hold:

$$T(\lambda, s(\lambda), d, n(\lambda), \kappa(\lambda)) = T^{meas}(\lambda). \quad (9)$$

This equation has two unknowns $n(\lambda)$ and $\kappa(\lambda)$ and, therefore, in general, its set of solutions is a curve in the two-dimensional $(n(\lambda), \kappa(\lambda))$ space. Therefore, the set of functions (n, κ) that satisfy (9) for a given d is infinite and, roughly speaking, is represented by a nonlinear manifold of dimension N in \mathbb{R}^{2N} .

However, physical constraints reduce drastically the range of variability of the unknowns $n(\lambda), \kappa(\lambda)$. For example, in the neighborhood of the fundamental absorption edge (normal dispersion), these physical constraints are:

PC1. $n(\lambda) \geq 1$ and $\kappa(\lambda) \geq 0$ for all $\lambda \in [\lambda_{\min}, \lambda_{\max}]$;

PC2. $n(\lambda)$ and $\kappa(\lambda)$ are decreasing functions of λ ;

PC3. $n(\lambda)$ is convex;

PC4. There exists $\lambda_{infl} \in [\lambda_{\min}, \lambda_{\max}]$ such that $\kappa(\lambda)$ is convex if $\lambda \geq \lambda_{infl}$ and concave if $\lambda < \lambda_{infl}$.

Observe that, assuming **PC2**, **PC1** is satisfied under the sole assumption $n(\lambda_{\max}) \geq 1$ and $\kappa(\lambda_{\max}) \geq 0$. The constraints **PC2**, **PC3**, and **PC4** can be written, respectively, as

$$n'(\lambda) \leq 0 \text{ and } \kappa'(\lambda) \leq 0 \quad \text{for all } \lambda \in [\lambda_{\min}, \lambda_{\max}], \quad (10)$$

$$n''(\lambda) \geq 0 \quad \text{for all } \lambda \in [\lambda_{\min}, \lambda_{\max}], \quad (11)$$

$$\kappa''(\lambda) \leq 0 \quad \text{for all } \lambda \in [\lambda_{\min}, \lambda_{infl}], \quad (12)$$

and

$$\kappa''(\lambda) \geq 0 \quad \text{for all } \lambda \in [\lambda_{infl}, \lambda_{\max}]. \quad (13)$$

Clearly, the constraints

$$n''(\lambda) \geq 0 \text{ for all } \lambda \in [\lambda_{\min}, \lambda_{\max}] \quad \text{and} \quad n'(\lambda_{\max}) \leq 0$$

imply that

$$n'(\lambda) \leq 0 \quad \text{for all } \lambda \in [\lambda_{\min}, \lambda_{\max}].$$

Moreover,

$$\kappa''(\lambda) \geq 0 \text{ for all } \lambda \in [\lambda_{infl}, \lambda_{\max}] \quad \text{and} \quad \kappa'(\lambda_{\max}) \leq 0$$

imply that

$$\kappa'(\lambda) \leq 0 \quad \text{for all } \lambda \in [\lambda_{infl}, \lambda_{\max}].$$

Finally,

$$\kappa''(\lambda) \leq 0 \text{ for all } \lambda \in [\lambda_{\min}, \lambda_{infl}] \quad \text{and} \quad \kappa'(\lambda_{\min}) \leq 0$$

imply that

$$\kappa'(\lambda) \leq 0 \quad \text{for all } \lambda \in [\lambda_{\min}, \lambda_{infl}].$$

Therefore, **PC2** can be replaced by

$$n'(\lambda_{\max}) \leq 0, \quad \kappa'(\lambda_{\max}) \leq 0, \quad \text{and} \quad \kappa'(\lambda_{\min}) \leq 0. \quad (14)$$

Summing up, the assumptions **PC1–PC4** will be satisfied if, and only if,

$$n(\lambda_{\max}) \geq 1, \quad \kappa(\lambda_{\max}) \geq 0, \quad (15)$$

$$n'(\lambda_{\max}) \leq 0, \quad \kappa'(\lambda_{\max}) \leq 0, \quad (16)$$

$$n''(\lambda) \geq 0, \quad \text{for all } \lambda \in [\lambda_{\min}, \lambda_{\max}], \quad (17)$$

$$\kappa''(\lambda) \geq 0, \quad \text{for all } \lambda \in [\lambda_{infl}, \lambda_{\max}], \quad (18)$$

$$\kappa''(\lambda) \leq 0, \quad \text{for all } \lambda \in [\lambda_{\min}, \lambda_{infl}], \quad (19)$$

and

$$\kappa'(\lambda_{\min}) \leq 0. \quad (20)$$

So, the continuous least squares solution of the estimation problem is the solution $(d, n(\lambda), \kappa(\lambda))$ of

$$\text{minimize } \int_{\lambda_{\min}}^{\lambda_{\max}} |T(\lambda, s(\lambda), d, n(\lambda), \kappa(\lambda)) - T^{meas}(\lambda)|^2 d\lambda \quad (21)$$

subject to the constraints (15)–(20).

Our idea in this work is to eliminate, as far as possible, the constraints of the problem, by means of a suitable change of variables. Roughly speaking, we are going to put the objective function (21) as depending on the second derivatives of $n(\lambda)$ and $\kappa(\lambda)$ plus functional values and first derivatives at λ_{\max} . Moreover, positivity will be guaranteed expressing the variables as squares of auxiliary unknowns. In fact, we write

$$n(\lambda_{\max}) = 1 + u^2, \quad \kappa(\lambda_{\max}) = v^2, \quad (22)$$

$$n'(\lambda_{\max}) = -u_1^2, \quad \kappa'(\lambda_{\max}) = -v_1^2, \quad (23)$$

$$n''(\lambda) = w(\lambda)^2 \quad \text{for all } \lambda \in [\lambda_{\min}, \lambda_{\max}], \quad (24)$$

$$\kappa''(\lambda) = z(\lambda)^2 \quad \text{for all } \lambda \in [\lambda_{infl}, \lambda_{\max}], \quad (25)$$

and

$$\kappa''(\lambda) = -z(\lambda)^2 \quad \text{for all } \lambda \in [\lambda_{\min}, \lambda_{infl}]. \quad (26)$$

At this point, in order to avoid a rather pedantic continuous formulation of the problem, we consider the real-life situation, in which data are given by a set of N equally spaced points on the interval $[\lambda_{\min}, \lambda_{\max}]$. So, we define

$$h = (\lambda_{\max} - \lambda_{\min}) / (N - 1),$$

and

$$\lambda_i = \lambda_{\min} + (i - 1)h \quad \text{for } i = 1, \dots, N.$$

Consequently, the measured transmission at λ_i will be called T_i^{meas} . Moreover, we will use the notation n_i, κ_i, w_i , and z_i for the estimates of $n(\lambda_i), \kappa(\lambda_i), w(\lambda_i)$, and $z(\lambda_i)$, for all $i = 1, \dots, N$. The discretization of the differential relations (22)–(26) gives

$$n_N = 1 + u^2, \quad v_N = v^2, \quad (27)$$

$$n_{N-1} = n_N + u_1^2 h, \quad \kappa_{N-1} = \kappa_N + v_1^2 h, \quad (28)$$

$$n_i = w_i^2 h^2 + 2n_{i+1} - n_{i+2} \quad \text{for } i = 1, \dots, N - 2, \quad (29)$$

$$\kappa_i = z_i^2 h^2 + 2\kappa_{i+1} - \kappa_{i+2}, \quad \text{if } \lambda_{i+1} \geq \lambda_{infl}, \quad (30)$$

and

$$\kappa_i = -z_i^2 h^2 + 2\kappa_{i+1} - \kappa_{i+2}, \quad \text{if } \lambda_{i+1} < \lambda_{infl}. \quad (31)$$

Finally, the objective function (21) is approximated by a sum of squares, giving the optimization problem

$$\text{minimize } \sum_{i=1}^N [T(\lambda_i, s(\lambda_i), d, n_i, \kappa_i) - T_i^{meas}]^2 \quad (32)$$

subject to

$$\kappa_1 \geq \kappa_2. \quad (33)$$

Since n_i and κ_i depend on u, u_1, v, v_1, w, z , and λ_{infl} through (27)–(31), problem (32) takes the form

$$\text{minimize } f(d, \lambda_{infl}, u, u_1, v, v_1, w_1, \dots, w_{N-2}, z_1, \dots, z_{N-2}) \quad (34)$$

subject to (33).

We expect that the constraint (33) will be inactive at a solution of (34)–(33), so we are going to consider the unconstrained problem (34). The constraint (33) can also be explicitly considered in the numerical procedure, by adding a penalty term $\rho \max\{0, \kappa_2 - \kappa_1\}^2$. Although our code is prepared to do that, this was never necessary in the experiments. The unknowns that appear in (34) have a different nature. The thickness d is a dimensional variable (measured in nanometers in our problems) that can be determined using the observations T_i^{meas} for (say) $\lambda_i \geq \lambda_{bound}$, where λ_{bound} , an upper bound for λ_{infl} , reflects our prior knowledge of the problem. For this reason, our first step in the estimation procedure will be to estimate d using data that correspond to $\lambda_i \geq \lambda_{bound}$. For accomplishing this objective we solve the problem

$$\text{minimize } \bar{f}(u, u_1, v, v_1, w, z) \equiv \sum_{\lambda_i \geq \lambda_{bound}} [T(\lambda_i, s(\lambda_i), d, n_i, \kappa_i) - T_i^{meas}]^2 \quad (35)$$

for different values of d and we take as estimated thickness the one that gives the lowest functional value. In this case the constraint (33) is irrelevant since it is automatically satisfied by the convexity of κ and the fact that the derivative of κ at λ_{min} is nonpositive. From now on we consider that d is fixed, coming from the procedure above.

The second step consists of determining λ_{infl} , together with the unknowns u, u_1, v, v_1, w, z . For this purpose observe that, given d and λ_{infl} , the problem

$$\text{minimize } \sum_{i=1}^N [T(\lambda_i, s(\lambda_i), d, n_i, \kappa_i) - T_i^{meas}]^2 \quad (36)$$

is (neglecting (33)) an unconstrained minimization problem whose variables are u, u_1, v, v_1, w , and z ($2N$ variables). We solve this problem for several trial values of λ_{infl} and we take as estimates of n and κ the combination of variables that gives the lowest value. For minimizing this function and for solving (35) for different trial thickness, we use the unconstrained minimization solver that will be described in the next section.

3. DESCRIPTION OF THE UNCONSTRAINED MINIMIZATION ALGORITHM

As we saw in the previous section, the unconstrained minimization problems (35) and (36) have the form

$$\text{minimize } f(u, u_1, v, v_1, w_1, \dots, w_{N-2}, z_1, \dots, z_{N-2}). \quad (37)$$

In order to simplify the notation, in this section we will write

$$x = (u, u_1, v, v_1, w_1, \dots, w_{N-2}, z_1, \dots, z_{N-2}).$$

Partial derivatives of f are usually necessary in optimization algorithms, since they provide the first-order information on the objective function that allows computational algorithms to follow downhill trajectories. In this case, derivatives are very hard to compute. For this reason it was necessary to use an automatic differentiation procedure (reverse mode) for performing this task. See [11] for details.

In principle, any unconstrained optimization algorithm can be used to solve (37) (see [12, 13]). Since the problem has, potentially, a large number of variables, our choice must be restricted to methods that are able to cope with that situation. A recent paper by Raydan [10] induced us to use the spectral gradient method (SGM), an implementation of the Barzilai–Borwein method for quadratics, introduced in [10]. In fact, Raydan showed, using a well known set of classical test problems, that SGM outperforms conjugate gradient algorithms (see [14, 13]) for large scale unconstrained optimization. Raydan’s spectral gradient method is extremely easy to implement, a fact that contributed to support our decision, since it enables us to become independent of black-box like imported software. Our description of SGM here is, essentially, the one of Raydan with a small difference in the choice of the step α_k when $b_k \leq 0$.

We denote $g(x) = \nabla f(x)$. The algorithm starts with $x_0 \in \mathbb{R}^n$ and uses an integer $M \geq 0$, a small parameter $\varepsilon > 0$, a sufficient decrease parameter $\gamma \in (0, 1)$, and safeguarding parameters $0 < \sigma_1 < \sigma_2 < 1$. Initially, $\alpha_0 \in [\varepsilon, 1/\varepsilon]$ is arbitrary. Given $x_k \in \mathbb{R}^n$, and $\alpha_k \in [\varepsilon, 1/\varepsilon]$, Algorithm 3.1 describes how to obtain x_{k+1} and α_{k+1} , and when to terminate the process.

ALGORITHM 3.1.

Step 1. *Detect whether the current point is stationary.*

If $\|g(x_k)\| = 0$, terminate the generation of the sequence, declaring that x_k is stationary.

Step 2. *Backtracking.*

Step 2.1. Set $\lambda \leftarrow \alpha_k$.

Step 2.2. Set $x_+ = x_k - \lambda g(x_k)$.

Step 2.3. If

$$f(x_+) \leq \max_{0 \leq j \leq \min\{k, M-1\}} \{f(x_{k-j})\} + \gamma \langle x_+ - x_k, g(x_k) \rangle, \quad (38)$$

then define $x_{k+1} = x_+$, $s_k = x_{k+1} - x_k$, and $y_k = g(x_{k+1}) - g(x_k)$.

Else, define

$$\lambda_{new} \in [\sigma_1 \lambda, \sigma_2 \lambda], \quad (39)$$

set $\lambda \leftarrow \lambda_{new}$, and go to Step 2.2.

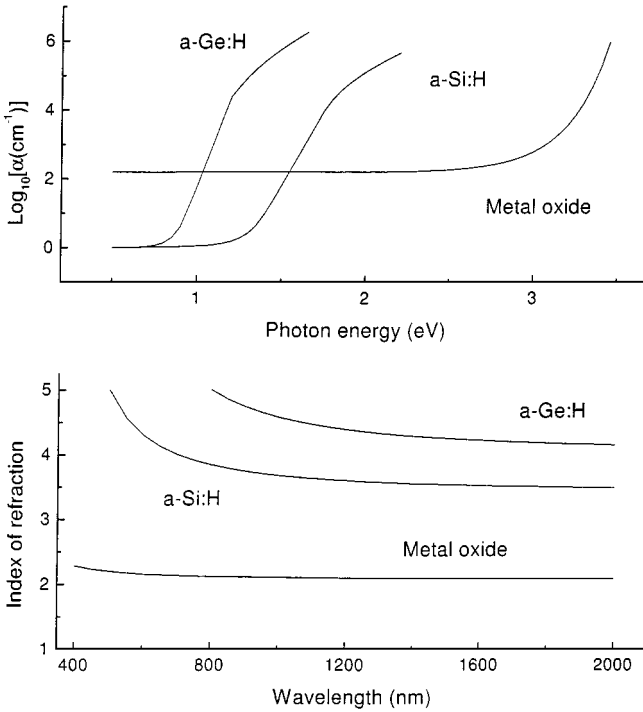


FIG. 1. Optical constants adopted for the simulation of thin films. See the corresponding analytical expressions in the Appendix.

Step 3. Compute spectral steplength.

Compute $b_k = \langle s_k, y_k \rangle$.

If $b_k \leq 0$, set $\alpha_{k+1} = \alpha_{\max}$,

else, compute $a_k = \langle s_k, s_k \rangle$, and

$$\alpha_{k+1} = \min\{\alpha_{\max}, \max\{\alpha_{\min}, a_k/b_k\}\}.$$

In practice the computation of λ_{new} uses one-dimensional quadratic interpolation and it is safeguarded with (39).

4. NUMERICAL RESULTS

In order to test the reliability of the new unconstrained optimization approach we used the computer-generated transmission of *gedanken* films deposited onto glass or crystalline silicon substrates. The expressions of $s_{\text{glass}}(\lambda)$ and $s_{\text{Si}}(\lambda)$, the refractive indices of the glass and the silicon substrates, respectively, are shown in the Appendix.

In all the simulations, we assume that the wavelength and the thickness are measured in nanometers. The transmission $T^{\text{true}}(\lambda)$ for each film was first computed in the range $\lambda \in [\lambda_{\min}, \lambda_{\max}]$ using a known thickness d^{true} , a known refractive index $n^{\text{true}}(\lambda)$, and a known absorption coefficient $\alpha^{\text{true}}(\lambda)$. In order to consider realistic situations, including experimental inaccuracy, the true transmission $T^{\text{true}}(\lambda)$ was rounded to four decimals. We performed numerical experiments using 100 transmission points. The precision obtained in d , $n(\lambda)$, and $\alpha(E)$ rounding the transmission data to four decimal places after the decimal point and without rounding was essentially the same.

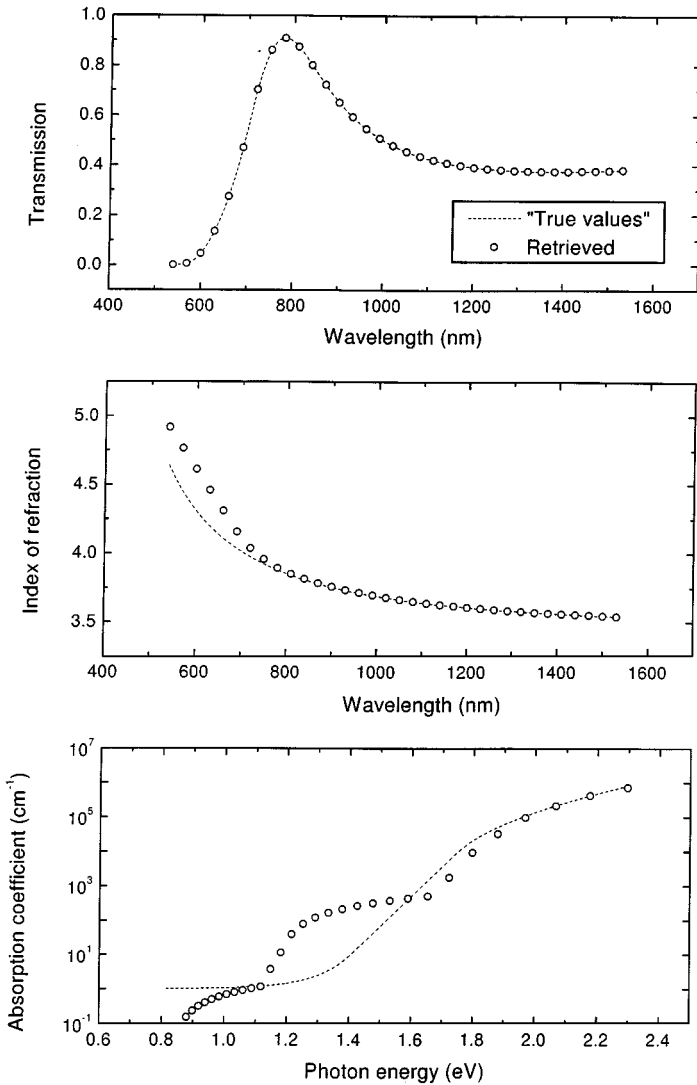


FIG. 2. “True” (dashed lines) and retrieved values (open circles) of the optical transmission, the refractive index, and the absorption coefficient of a numerically generated thin film of thickness $d = 100$ nm simulating an a-Si:H layer deposited on glass (*Film A*). Note the good agreement found for the optical constants despite the thinness of the film.

Three different materials, hydrogenated amorphous silicon (a-Si:H), hydrogenated amorphous germanium (a-Ge:H), and a *gedanken* metal oxide, were simulated. The numerical experiments consider three thicknesses: 80, 100, and 600 nm. The trial films are “deposited” on a glass or on a c-Si substrate. Note that the transmission formula (3) being used assumes that the substrate is perfectly transparent. As a consequence of this limitation, the useful spectral ranges 350–2000 nm for glass and 1250–2600 nm for c-Si substrates have been retained in the numerical experiments. The expressions of $\alpha^{true}(E)$ and $n^{true}(\lambda)$ used to generate the transmission spectra are shown in the Appendix. Their dependence on photon energy (E) and wavelength, respectively, are displayed in Fig. 1. The description of the five *gedanken* experiments and the retrieved numerical results follow.

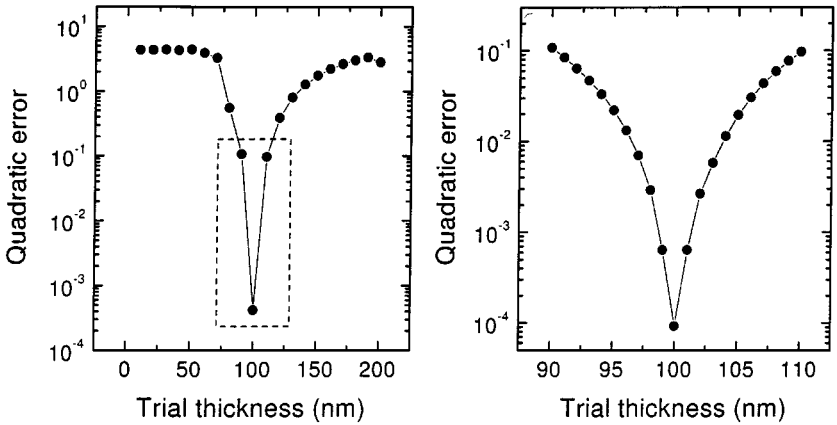


FIG. 3. Quadratic error of the minimization process as a function of trial thickness for *Film A*. On the left side the trial thickness step is 10 nm whereas on the right hand side of the figure the refined trial step is 1 nm. Note the excellent retrieval of the film thickness after 5000 iterations.

Film A. This computer-generated film simulates an a-Si:H thin film deposited on a glass substrate with $d^{true} = 100$ nm. The computed transmission $T^{true}(\lambda)$ in the 540–1530 nm wavelength range, and the optical constants $n^{true}(\lambda)$ and $\alpha^{true}(E)$ are shown as dashed lines in Fig. 2. The retrieved values of $T^{true}(\lambda)$, $n^{true}(\lambda)$, and $\alpha^{true}(E)$ are represented in the same figure as open circles. The retrieval of the film thickness is shown in Fig. 3. A few comments are in order. First, the transmission spectrum does not show any fringe pattern in the calculated spectral range, as expected for a 100-nm thin film. A well defined maximum at approximately $\lambda = 780$ nm and no well defined minima are apparent from Fig. 2. In spite of this, the “true” thickness is retrieved with a surprising precision. Second, within most of the analyzed spectral range $n^{true}(\lambda)$ and $n^{retr}(\lambda)$ are in very good agreement. At short wavelengths a small difference appears (of up to 0.05) between $n^{true}(\lambda)$ and the retrieved $n(\lambda)$. Third, within a factor of two or three, the absorption coefficient is correctly retrieved in a 3.5 orders of magnitude dynamical range. The retrieval of true values, however, fails for $\alpha < 500$ cm^{-1} . Remember that the simulation refers to a 100-nm thick film. We consider the overall retrieval of the thickness and the optical constants to constitute an outstanding result.

Film B. This computer-generated film is identical to *Film A* except for its thickness $d^{true} = 600$ nm. The transmission spectrum displays a well structured fringe pattern, as shown in Fig. 4. The retrieved values $T^{retr}(\lambda)$, $n^{retr}(\lambda)$, and $\alpha^{retr}(E)$ are also indicated in Fig. 4 (open circles). Figure 5 shows the results of the minimization process for steps of 10 nm and 1 nm. The true thickness has been perfectly retrieved. In fact, the overall retrieval is almost perfect in this case. In particular, the absorption coefficient has been correctly retrieved for a dynamical range of more than 5 orders of magnitude, down to $\alpha \approx 1$ cm^{-1} . The results shown in Figs. 2 and 4 confirm the well known fact that the thicker the film, the easier it is to retrieve a small absorption coefficient.

Film C. This computer-generated film simulates a $d^{true} = 100$ nm hydrogenated amorphous germanium thin film deposited on a crystalline silicon substrate. The computed transmission $T^{true}(\lambda)$, as well as $n^{true}(\lambda)$ and $\alpha^{true}(E)$, is shown as dashed lines in Fig. 6. $T^{true}(\lambda)$ has been calculated in the (relatively narrow) spectral region 1250–2537 nm where c-Si is transparent. As in the case of *Film A*, there is not a well defined fringe pattern.

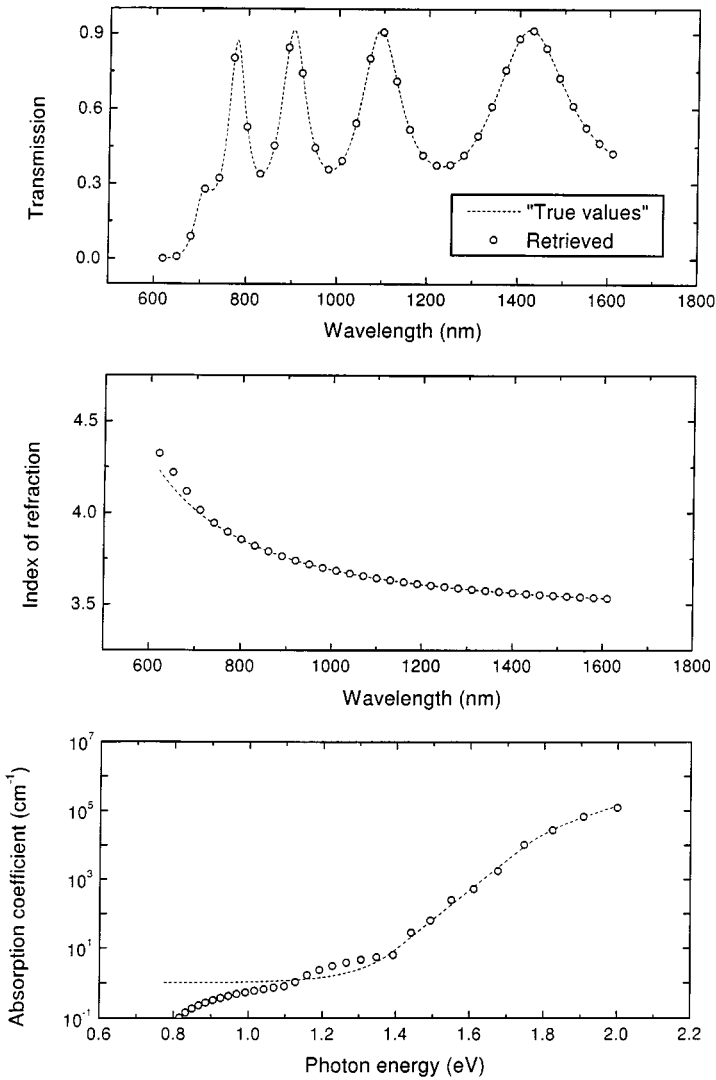


FIG. 4. “True” (dashed lines) and retrieved values (open circles) of the transmission, the refractive index, and the absorption coefficient of a numerically generated film of thickness $d = 600$ nm simulating an a-Si:H layer deposited on glass (*Film B*). Note the very good agreement found for the optical constants and the transmission.

However, two important differences between *Film A* and *Film C* have to be noted here: (i) the index of refraction difference between film and substrate is much larger in the former than in the latter case, and (ii) the spectral region computed for *Film C* does not include large absorption coefficient values. In other words, *Film C* is more “transparent” in the wavelength range considered in the retrieval process. The transmission of *Film C* displays a well defined minimum at $\lambda \approx 1520$ nm but a neighboring maximum does not appear in the computed spectral range. The result of the film thickness retrieval process appears in Fig. 7. In this case, the overall retrieval process is not as good as in the preceding cases. In particular the retrieval of the absorption coefficient is poor. We believe this to be due to the thinness of the film allied to the fact that the spectral region under consideration does not include large absorption coefficients, i.e., $\alpha > 100$ cm⁻¹. This constitutes the worst imaginable

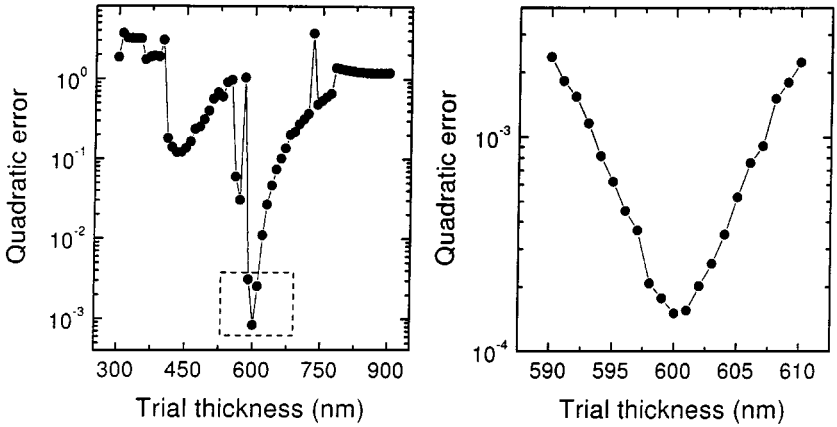


FIG. 5. Quadratic error of the minimization process as a function of trial thickness for *Film B*. On the left side the trial thickness step is 10 nm whereas on the right hand side of the figure the refined trial step is 1 nm (5000 iterations). Note the excellent retrieval of the film thickness and the local-nonglobal minimizers.

situation, a very thin non-absorbing film. In spite of this, the “true” thickness has been retrieved (see Fig. 7), as well as the index of refraction (see Fig. 6). We conclude that the algorithm under discussion fails to retrieve small absorption coefficients of very thin films when the transmission spectrum contains data referring only to almost transparent regions.

Film D. This computer-generated film is identical to *Film C* except for its thickness $d^{true} = 600$ nm. The transmission spectrum as well as the “true” and retrieved optical constants are shown in Fig. 8. Figure 9 displays the results of the minimization process leading to the “true” 600 nm thickness. Note that for this thicker a-Ge:H film deposited onto c-Si the retrieval of d and $n(\lambda)$ is perfect (see Fig. 8), as well as the “true” absorption coefficient down to 1 cm^{-1} . However, the retrieval of α fails for $E < 0.7$ eV. In the small α region of the spectrum, these findings mimic those obtained with *Film B* (Fig. 4).

Film E. The last numerical example simulates a metal oxide film ($d^{true} = 80$ nm) deposited onto glass. The computed transmission spectrum in the 360–657 nm wavelength range used for the retrieval of the thickness and the optical constants of the material is shown in Fig. 10. Figure 10 also displays the retrieved values of n and α . The film thickness was perfectly retrieved, as shown in Fig. 11. Let us note at this point the following: (i) the film thinness and the similar n values of both film and substrate inhibit the appearance of a fringe pattern, (ii) in spite of this fact the optical constants and d are very well retrieved, and (iii) additional numerical experiments show that for $50 < d < 75$ nm thick films, the present algorithm fails to retrieve d , n , and α with a precision better than around 10%.

Table I summarizes the findings of all the reported numerical experiments. We finish this section providing details of our numerical procedure.

For our calculations we need initial estimates of $\kappa(\lambda)$ and $n(\lambda)$. As initial estimate of $\kappa(\lambda)$ we used a piecewise linear function the values of which are 0.1 at the smallest wavelength of the spectrum, 0.01 at $\lambda_{\min} + 0.2(\lambda_{\max} - \lambda_{\min})$, and 10^{-10} at λ_{\max} . The initial estimates of $n(\lambda)$ are linear functions varying between 5 (λ_{\min}) and 2 (λ_{\max}) with step 1 (these values were chosen because of the previous knowledge of the simulated materials). We excluded the constant functions because preliminary tests showed us they lead the method to local minimizers. So, we have six possibilities for the initial estimate of $n(\lambda)$: the decreasing linear functions

TABLE I
Thickness Estimation

Film	Spectra	d^{true}	d^{retr}	Quadratic error
A	540–1530	100	100	6.338394×10^{-6}
B	620–1610	600	600	2.425071×10^{-5}
C	1250–2537	100	100	6.094629×10^{-8}
D	1250–2537	600	600	6.353207×10^{-8}
E	360–657	80	80	5.085419×10^{-7}

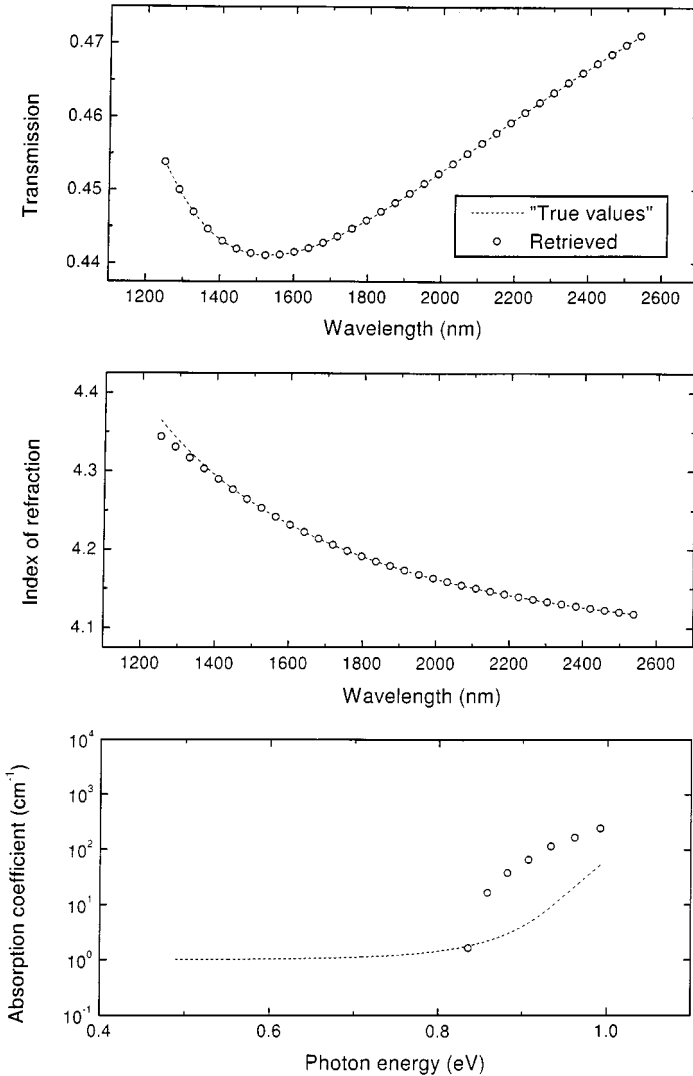


FIG. 6. “True” (dashed lines) and retrieved values (open circles) of the transmission, the refractive index, and the absorption coefficient of a numerically generated $d = 100$ nm thick film simulating an a-Ge:H layer deposited on a crystalline silicon substrate (*Film C*). Note that in the spectral region where the c-Si substrate is transparent the a-Ge:H is weakly absorbing. A good retrieval is found for the index of refraction and for the transmission, which does not display any fringe pattern. However, the algorithm failed (within an order of magnitude) to retrieve the correct absorption coefficient in the $1 < \alpha < 100$ cm⁻¹ interval.

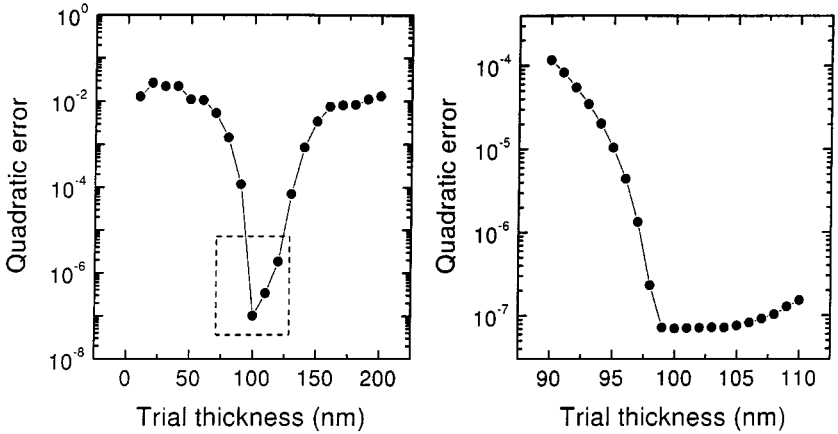


FIG. 7. Quadratic error of the minimization process as a function of trial thickness for *Film C*. On the left side the trial thickness step is 10 nm whereas on the right hand side of the figure the refined trial step is 1 nm (5000 iterations). The “true” thickness of the film has been retrieved.

defined by the pairs of points $[(\lambda_{\min}, 3); (\lambda_{\max}, 2)]$, $[(\lambda_{\min}, 4); (\lambda_{\max}, 2)]$, $[(\lambda_{\min}, 5); (\lambda_{\max}, 2)]$, $[(\lambda_{\min}, 4); (\lambda_{\max}, 3)]$, $[(\lambda_{\min}, 5); (\lambda_{\max}, 3)]$, and $[(\lambda_{\min}, 5); (\lambda_{\max}, 4)]$. The reported computed $n(\lambda)$ corresponds to the best performance.

The general scheme to obtain the optimal parameters is as follows. First, we need to break down the spectrum into two parts: $[\lambda_{\min}, \lambda_{bound}]$ and $[\lambda_{bound}, \lambda_{\max}]$, where λ_{bound} is a known upper bound of λ_{inft} . To estimate the thickness we use the points with abscissa belonging to $[\lambda_{bound}, \lambda_{\max}]$. The procedure consists in running Algorithm 3.1 for different values of d between $d^{\min} = \frac{1}{2}d^{kick}$ and $d^{\max} = \frac{3}{2}d^{kick}$ with step 10, $(d^{\min}, d^{\min} + 10, d^{\min} + 20, \dots)$, where d^{kick} is a rough initial estimate of the true thickness. In this way, we obtain d^{trial} , the thickness value for which the smallest quadratic error occurs. Then we repeat the procedure with $d^{\min} = d^{trial} - 10$, $d^{\max} = d^{trial} + 10$ and step 1 obtaining, finally, the estimated thickness d^{best} .

To estimate the inflection point we proceed in an analogous way, using the whole spectrum and the thickness fixed at d^{best} , trying different possible inflection points (obviously between λ_{\min} and λ_{bound}) and taking as the estimated inflection point the one which gives the smallest quadratic error. In all the runs just described, we allow only 3000 and 5000 iterations of Algorithm 3.1, when the d^{trial} step is equal to 10 and 1, respectively. The final step of the method consists on fixing d^{best} and λ_{inft} , and running Algorithm 3.1 once more allowing 50,000 iterations.

All the experiments were run in a SPARCstation Sun Ultra 1, with an UltraSPARC 64 bits processor, 167-MHz clock, and 128 MBytes of RAM memory. We used the language C++ with the g++ compiler (GNU project C and C++ compiler v 2.7) and the optimization compiler option `-O4`. In spite of the many executions of the unconstrained minimization algorithm that are necessary to solve each problem, the total CPU time used under the mentioned computer environment never exceeded 5 minutes.

5. CONCLUSIONS

The analysis of the numerical results allows us to draw the following conclusions.

1. The proposed procedure is highly reliable for estimating the true thickness in all films when four digits transmission data are used. The method provides a very good retrieval

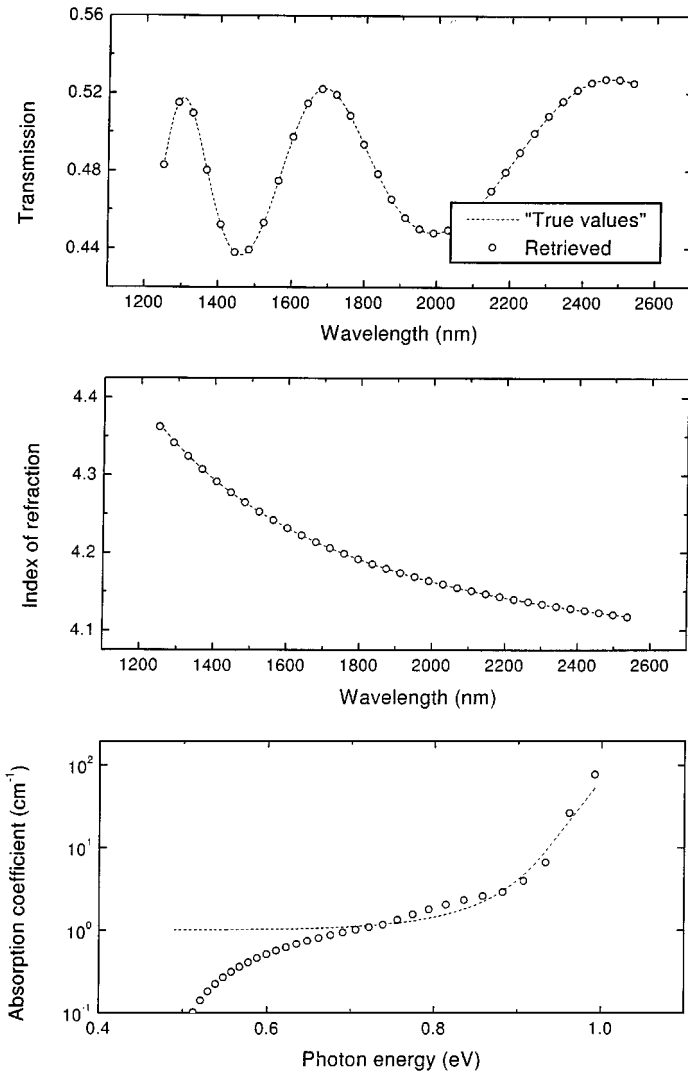


FIG. 8. “True” and retrieved values of the transmission, the refractive index, and the absorption coefficient of a numerically generated thin film of thickness $d = 600$ nm simulating an a-Ge:H layer deposited on a crystalline silicon substrate (*Film D*). Note the overall good agreement found for the optical constants and the transmission. The retrieval of the “true” absorption coefficient for $1 < \alpha < 100$ cm^{-1} is excellent.

of the true transmission in cases where no approximate methods are useful, i.e., very thin films ($d > 75$ nm) or absorbing layers.

2. The algorithm being discussed here fails to retrieve the true thickness and the true absorption coefficient from the transmission spectrum of very thin transparent films. Additional numerical experiments, not being discussed here, indicate a defective retrieval of the thickness and the optical constants of $d < 75$ nm thin films from optical transmission data.

3. In some cases the quadratic error as a function of the guessed thickness (Fig. 5) is a function with several local-nonglobal minimizers. The strategy of separating the variable d from the other variables of the optimization problem appears to be correct, since it tends to avoid spurious convergence to those local minimizers.

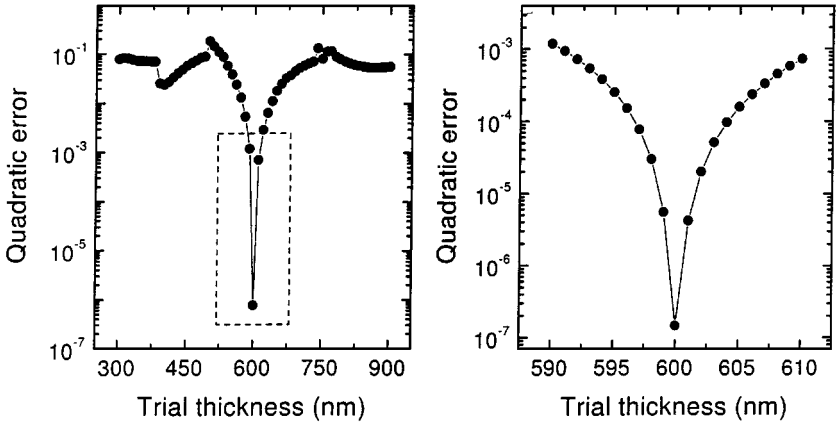


FIG. 9. Quadratic error of the minimization process as a function of trial thickness for *Film D*. On the left side the trial thickness step is 10 nm whereas on the right hand side of the figure the refined trial step is 1 nm (5000 iterations). Note the excellent retrieval of the film thickness and the local-nonglobal minimizers.

4. The comparison of the present results with those previously obtained using the algorithm described in [5, 6] seems to confirm that the new method is, at least, as efficient as the previous constrained optimization approach. In addition, the resulting piece of software is more portable and easier to manipulate.

5. As one of the referees pointed out, further time reductions can be expected from considering spectral preconditioning schemes (see [15]). This will be done in future works.

APPENDIX

Analytical expressions used to compute the substrates and the simulated optical constants of semiconductor and dielectric films are

$$s_{\text{glass}}(\lambda) = \sqrt{1 + (0.7568 - 7930/\lambda^2)^{-1}}, \quad (40)$$

$$s_{\text{Si}}(\lambda) = 3.71382 - 8.69123 \cdot 10^{-5}\lambda - 2.47125 \cdot 10^{-8}\lambda^2 + 1.04677 \cdot 10^{-11}\lambda^3. \quad (41)$$

a-Si:H

Index of refraction,

$$n^{\text{true}}(\lambda) = \sqrt{1 + (0.09195 - 12600/\lambda^2)^{-1}}. \quad (42)$$

Absorption coefficient,

$$\ln(\alpha^{\text{true}}(E)) = \begin{cases} 6.5944 \cdot 10^{-6} \exp(9.0846E) - 16.102, & 0.60 < E < 1.40; \\ 20E - 41.9, & 1.40 < E < 1.75; \\ \sqrt{59.56E - 102.1} - 8.391, & 1.75 < E < 2.29. \end{cases} \quad (43)$$

a-Ge:H

Index of refraction,

$$n^{\text{true}}(\lambda) = \sqrt{1 + (0.065 - (15000/\lambda^2)^{-1}}. \quad (44)$$

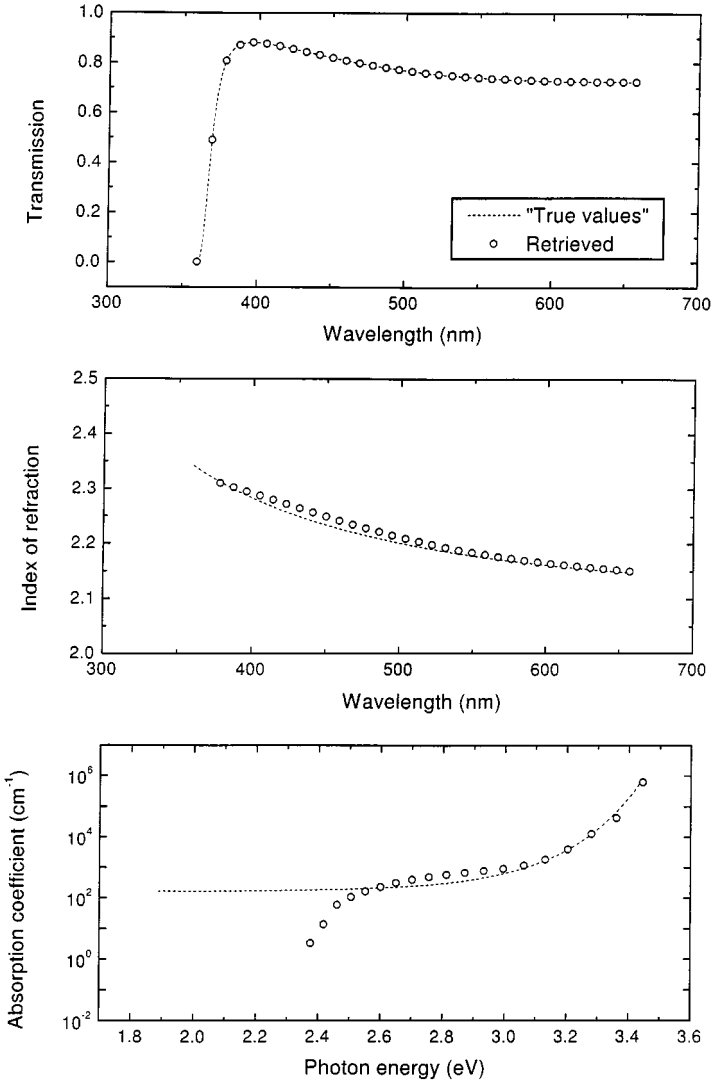


FIG. 10. “True” and retrieved values of the transmission, the refractive index, and the absorption coefficient of a numerically generated thin film of thickness $d = 80$ nm simulating a metal oxide layer deposited on glass (*Film E*). The overall retrieval of the optical constants and the transmission is excellent. Note that (i) the transmission spectrum does not contain any interference fringe pattern, and (ii) the “true” absorption coefficient has been correctly retrieved for a four orders of magnitude dynamical range. However, the retrieval of α fails for $E < 2.45$ eV.

Absorption coefficient,

$$\ln(\alpha^{true}(E)) = \begin{cases} 6.5944 \cdot 10^{-6} \exp(13.629E) - 16.102, & 0.48 < E < 0.93; \\ 30E - 41.9, & 0.93 < E < 1.17; \\ \sqrt{89.34E - 102.1} - 8.391, & 1.17 < E < 1.50. \end{cases} \quad (45)$$

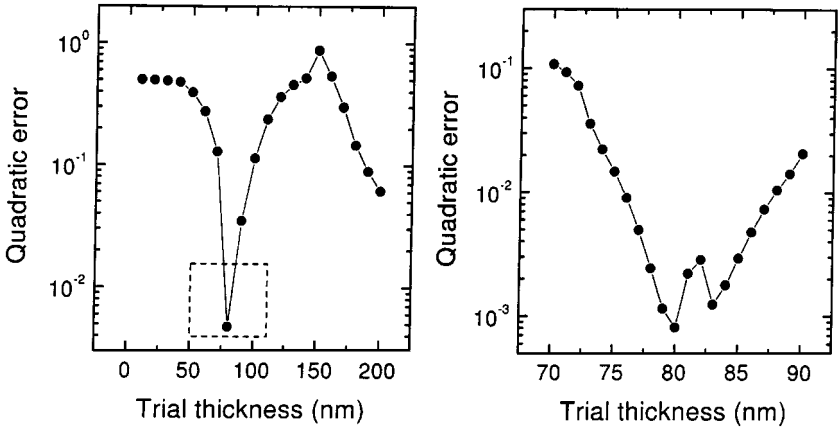


FIG. 11. Quadratic error of the minimization process as a function of trial thickness for *Film E*. On the left side the trial thickness step is 10 nm whereas on the right hand side of the figure the refined trial step is 1 nm (5000 iterations). The “true” 80-nm thickness of the metal oxide layer was retrieved with no error.

Metal Oxide

Index of refraction,

$$n^{true}(\lambda) = \sqrt{1 + (0.3 - (10000/\lambda^2))^{-1}}. \quad (46)$$

Absorption coefficient,

$$\ln(\alpha^{true}(E)) = 6.5944 \cdot 10^{-6} \exp(4.0846E) - 11.02, \quad 0.5 < E < 3.5. \quad (47)$$

In the expressions above, the wavelength λ is in nm, the photon energy $E = 1240/\lambda$ is in eV, and the absorption coefficient α is in nm⁻¹.

ACKNOWLEDGMENTS

This work has been partially supported by the Brazilian agencies CNPq and FAPESP (Grants 90/3724, 96/5240, and 95/2452-6). The authors also acknowledge support from FINEP and FAEP-UNICAMP.

REFERENCES

1. M. Born and E. Wolf, *Principles of Optics* (Pergamon, London, 1980).
2. O. S. Heavens, *Optical Properties of Thin Films* (Dover, New York, 1991).
3. J. C. Manificier, J. Gasiot, and J. P. Fillard, A simple method for the determination of the optical constants n , k and the thickness of a weakly absorbin film, *J. Phys. E* **9**, 1002 (1976).
4. R. Swanepoel, Determination of the thickness and optical constants of amorphous silicon, *J. Phys. E* **16**, 1214 (1983).
5. R. Swanepoel, Determination of surface roughness and optical constants of inhomogeneous amorphous silicon films, *J. Phys. E* **17**, 896 (1984).
6. I. Chambouleyron, J. M. Martínez, A. C. Moretti, and M. Mulato, Retrieval of optical constants and thickness of thin films from transmission spectra, *Appl. Opt.* **36**, 8238 (1997).

7. I. Chambouleyron, J. M. Martínez, A. C. Moretti, and M. Mulato, Optical constants of thin films by means of a pointwise constrained optimization approach, *Thin Solid Films* **317**, 133 (1998).
8. B. A. Murtagh and M. A. Saunders, *MINOS User's Guide*, Report SOL 77-9, Department of Operations Research, Stanford University, CA, 1977.
9. B. A. Murtagh and M. A. Saunders, Large-scale linearly constrained optimization, *Math. Program.* **14**, 41 (1978).
10. M. Raydan, The Barzilai and Borwein gradient method for the large scale unconstrained minimization problem, *SIAM. J. Optim.* **7**, 26 (1997).
11. E. G. Birgin, *Computational Differentiation and Applications*, Ph.D. Thesis, Department of Applied Mathematics, IMECC-UNICAMP, 1998.
12. J. E. Dennis, Jr., and R. B. Schnabel, *Numerical Methods for Unconstrained Optimization and Nonlinear Equations* (Prentice-Hall, Englewood Cliffs, NJ, 1983).
13. P. E. Gill, W. Murray, and M. H. Wright, *Practical Optimization* (Academic Press, London, 1981).
14. R. Fletcher, *Practical Methods of Optimization*, 2nd ed. (Wiley, Chichester/New York, 1987).
15. F. Luengo, M. Raydan, W. Glunt, and T. L. Hayden. *Preconditioned Spectral Gradient Method for Unconstrained Optimization Problems*, Technical Report 96-08, Escuela de Computación, Facultad de Ciencias. Universidad Central de Venezuela, 47002 Caracas 1041-A, Venezuela, 1996.